Transworld Research Network
37/661 (2), Fort P.O., Trivandrum-695 023, Kerala, India

Thin Solid Films: Process and Applications, 2008: 189-227 ISBN: 978-81-7895-314-4
Editor: S.C. Nam

5 TiO_2 thin films for photocatalytic applications

K. Eufinger[1], D. Poelman[2], H. Poelman[2], R. De Gryse[2] and G.B. Marin[3]
[1]Centexbel-Gent, Zwijnaarde, Belgium; [2]Department of Solid State Sciences Ghent University, Gent, Belgium; [3]Laboratorium voor Petrochemische Techniek, Department of Chemical Engineering, Ghent University Gent, Belgium

Abstract

TiO_2 is a wide band gap semiconductor which has become well known as photoactivated catalyst for water and air purification and self cleaning surfaces. When illuminated with ultra-band gap ultraviolet (UV) light, electron-hole pairs are generated. To be utilized, the charge carriers need to migrate to the surface of the thin film, where they can initiate redox reactions such as the breakdown of organic pollutants. The charge carriers can also become trapped at defect sites in the material, which enhances their chance of recombination so that they are lost to the process. As a result, the photocatalytic activity of TiO_2 depends

Correspondence/Reprint request: Dr. D. Poelman, Department of Solid State Sciences, Ghent University, Gent Belgium. E-mail: Dirk.Poelman@UGent.be

on several factors, including the surface area and the number of defect states. In turn, these are determined by the stoichiometry, the degree of crystallinity and the crystallite size. Another important factor is the film thickness: Depending on the film morphology and the light source used a critical thickness is observed below which there is a strong dependence of the photocatalytic activity on the film thickness and above which the dependence is much smaller. The influences of surface area and film thickness are often underestimated and in many cases even neglected when comparing different thin films. A major issue is also the lack of a suitable reference thin film, which exists for powder TiO_2 catalysts in the form of Degussa P25.

In this paper we will give an overview of the state of the art in photocatalytic TiO_2 thin film deposition, with a special emphasis on direct current (d.c.) magnetron sputtering as deposition technique. In this context we will also discuss important issues that need to be taken into account when comparing different thin films.

1. Introduction

The importance of TiO_2 as a photocatalytic material was discovered by Fujishima and Honda in 1972, who observed the photocatalytic splitting of water on TiO_2 electrodes [1]. In the photocatalytic process TiO_2 is activated by illumination with (UV) light having an energy higher than the band gap. Given a band gap of $E_g = 3.2$ eV for anatase and 3.0 eV for rutile [2] this corresponds to wavelengths below 387 and 413 nm, respectively. The photocatalytic breakdown reaction proceeds via intermediate steps ending in the mineralization of the organic to water, CO_2 and mineral acids. The initial step is the electron-hole pair formation, followed by their separation. The electrons can be used for reduction, the holes for oxidation processes [2]. The lifetimes of the electron and the hole have an influence on how well they can be utilized for the subsequent redox reaction. Structural imperfections in the TiO_2 lattice generate trap sites and recombination centers, leading to a decrease of the electron and hole concentration [3-5].

In recent years, applications to environmental clean up have been one of the most active areas in heterogeneous photocatalysis [4-8]. Here one looks at the photo-degradation of hydrocarbons either in water or in air using suspended small particles or thin films of TiO_2. There are several advantages of this material over other photocatalytically active semiconductors: TiO_2 is low cost, chemically inert, absolutely non-toxic, highly photoactive, as well as self-regenerating and can easily be recycled [4]. Additionally, the redox potential of the H_2O/ $*OH$ couple (-2.8 eV) lies within its band gap energy [2], so that it can be used for water splitting.

TiO_2 has several naturally occurring modifications, the most common ones being rutile, anatase and brookite. Most research with respect to photocatalysis is performed using anatase [4-8], while in all other aspects rutile has been much more thoroughly characterized (e.g. electronic behavior, bulk structural investigations). This is mostly due to the preparation methods: While it is easier to obtain anatase than rutile at low temperatures below 600°C, it is impossible to obtain anything but rutile at temperatures above 800°C, the transition temperature to the thermodynamically most stable phase rutile [4]. Latter is the case during standard ceramic processing which requires temperatures of up to 1700°C. Very little is known about the brookite phase.

While TiO_2 powders or films obtained at low temperatures are finely grained (nanocrystalline) because little grain growth can occur, grain growth at temperatures above 800°C can be substantial. Therefore, depending on the preparation method, the nature of the TiO_2 particle or film surface, as well as the active surface area are usually very different for anatase and rutile powders. Since for a catalyst its active surface area is important, differences in surface area must be taken into account when comparing the activity of different materials.

Generating a larger surface area for a TiO_2 powder or thin film requires reducing the grain size. Most photocatalytic materials are nanocrystalline, i.e. having a grain or crystallite size below 100 nm. When the crystallite size decreases below about 10 nm, grain boundaries, which present a defective lattice, start to dominate the material. Defects in the lattice structure are detrimental to the photocatalytic activity as they act as trap sites for the photogenerated charge carriers, increasing their probability of recombination. This is why the highly defective amorphous state is expected to show no significant or only a very low photocatalytic activity, [4, 5, 7, 9]. Studies have shown, though, that TiO_2 which does not show any X-ray diffraction pattern (and is thus called XRD amorphous) shows very small crystalline domains when investigated with transmission electron microscopy (TEM) [10]. In general, amorphous TiO_2 has been studied little.

Originally, TiO_2 was applied in powder form for water cleaning. The difficulty to separate the powder from the water and expanding the applications to air cleaning resulted in using thin films of immobilized powder or directly deposited TiO_2. The complete reactor walls can be coated to act as photocatalytically active surfaces, but it has to be ensured that the complete catalyst surface is illuminated. Additionally, it is not always practical to coat the reactor walls. Therefore, often a coated sample area is tested inside the reactor. Since thin films are fixed to the substrate, they will not have an as large active surface area compared to that of a suspended powder.

There are different methods for thin film deposition which can be divided into two general areas, namely wet chemical and vapor deposition. The wet chemical technique employed most often is sol-gel [4, 11]. In earlier years the limitations of this wet process were due to the fact that the films had to be calcined at temperatures between 500-600°C, in order to achieve good stoichiometry and crystallinity. More recent investigations showed that these high temperatures were due to the wrong substrate choice (soda-lime glass) and caused by Na-contamination of the films [12]. Further development of the sol-gel technique has led to procedures which can yield crystalline TiO_2 powders at temperatures lower than 200°C [13]. For good bonding of a sol-gel film to a glass substrate, temperatures above 400°C are still necessary, though [4].

Chemical vapor deposition (CVD) and physical vapor deposition (PVD), including electron beam evaporation and (magnetron) sputtering [14] are frequently used vapor deposition techniques. With CVD powders as well as thin films can be synthesized, depending on the processing conditions. Physical vapor deposition techniques are used exclusively for thin film deposition. The main advantage of vapor deposition techniques, especially PVD, is that good adhesion of the film to the substrate can be achieved. A second advantage is that the process conditions can be controlled to yield crystalline thin films without extended external substrate heating.

In this review we will first give an introduction to the activity of TiO_2 (section 2) and discuss the important factors determining the photocatalytic activity of a thin film (section 3). Then we will give an overview of the different techniques used for TiO_2 thin film deposition (section 4) and using the example of d.c. magnetron sputtering from ceramic TiO_{2-x} targets we will point out how to deposit TiO_2 thin films with a high photocatalytic activity (section 5). In the end we will formulate some general considerations when testing the photocatalytic activity of TiO_2 thin films (section 6). The issue of doping, which is used to modify the electronic properties and thus the photocatalytic activity of TiO_2 will not be addressed as it is beyond the scope of this review. A detailed discussion can be found in [15].

2. Photocatalytic activity of TiO_2

Photocatalytic reactions are a special type of catalyzed chemical reactions which proceed under the involvement of light. When the catalyst is a semiconductor like TiO_2, this is called *semiconductor photocatalysis*. When the semiconductor (TiO_2) is activated by light electron-hole pairs are generated, and the electrons and holes can be utilized for electron transfer (redox) reactions at the surface of the semiconductor. All possible processes are summarized in Figure 1.

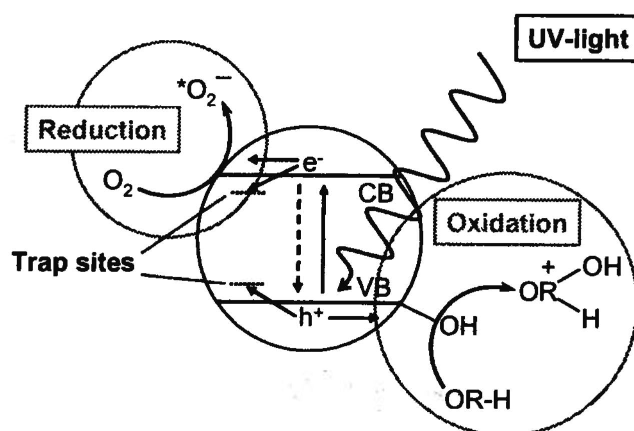

Figure 1. Scheme of the photocatalytic breakdown reaction of an organic molecule (OR) on the surface of a photoactivated semiconductor.

2.1. Photoactivation of TiO_2

Irradiation of the semiconductor TiO_2 with light having an energy larger than the band gap ($E \geq E_{bg}$) will generate electron-hole pairs, followed by their separation:

$$TiO_2 \xrightarrow{h\nu} TiO_2(e^-/h^+) \rightarrow e^-_{cb} + h^+_{vb} \quad (1)$$

As shown in Figure 1 the separated electrons and holes can migrate to the sample surface, where the electrons are available for reduction, the holes for oxidation processes [2]. The electrons are associated with the Ti^{4+} (forming Ti^{3+}), but they are immediately scavenged by adsorbed oxygen, resulting in the reduction of the latter. As a result, the lifetime of the Ti^{3+} states is very short, so that the TiO_2 is never truly in a reduced state [7]. The holes are associated mostly with –OH groups present at the surface due to saturation of the terminating O with water molecules from the ambient air. Also O^- and O_3^- are suggested as hole trap sites [4, 6, 7], the latter being formed from chemisorbed O_2. The resulting radicals oxidize the adsorbed organic compound(s) while being reduced themselves. The lifetimes of the electron and the hole determine their efficiency for the subsequent redox reaction. Structural imperfections in the TiO_2 lattice generate trap sites and recombination centers, leading to a decrease of the electron and hole concentration [3-5].

2.2. Photocatalytic (breakdown) reactions

We now look at the potentials of the electrons and holes generated by photoactivation in TiO_2. The electrons have a reduction potential reflected by the energy level of the bottom of the conduction band, while the holes have an oxidizing potential reflected by the top of the valence band. Therefore, the redox potential of the redox couple to be catalyzed must be situated between these two

energy levels, i.e. within the band gap of the semiconductor [2, 4, 8]. In the case of reactions in water, the positions of the band edges can be referred to the normal hydrogen electrode (NHE) [2], which is also a reference for the redox couples of chemical reactions in water. The redox potential, though, is influenced by the pH of the solution, which can also influence the surface of the solid semiconductor. For reactions in the gas phase no standards such as the NHE have been defined. Here, among others, the value of the redox potential difference will depend on the extent of interaction between the two phases, including the degree of chemisorption, the gas pressure and humidity.

The photocatalytic breakdown reaction of an organic compound normally proceeds via intermediate steps, ending in the mineralization of the organic to CO_2, water and mineral acids, summarized by equation (2):

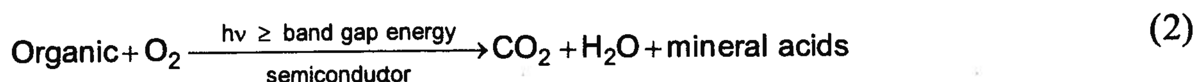

$$\text{Organic} + O_2 \xrightarrow[\text{semiconductor}]{h\nu \geq \text{band gap energy}} CO_2 + H_2O + \text{mineral acids} \quad (2)$$

Mineral acids are generated if there are any hetero-atoms, such as S, N, and Cl present in the organic. This catalytic process is exergonic (i.e. the free Gibbs enthalpy $\Delta G < 0$) and the energy of the photons is not used in the reaction other than to excite the catalyst. As discussed in the previous paragraph, the band gap and the position of the band edges of the semiconductor determine which breakdown reactions it can catalyze [2].

Other examples of photocatalytic 'breakdown' reactions are partial oxidation reactions, of e.g. alcohols to aldehydes or ketones, which can also be seen as synthesis of new organic molecules. This includes photocatalytically assisted polymerization [16]. A good overview of the different possible reactions is given in [4]. These processes should not be confused with the endergonic (non-spontaneous) synthesis (i.e. photosynthesis) of organic molecules which occurs in biological processes.

3. Structural factors controlling the photocatalytic activity of thin films

A TiO_2 film normally consists of crystalline grains which are characterized by their crystal phase, size, shape and arrangement on the substrate. As a result it can be expected to show a broad range of defects. In this section we will discuss the influence of individual defects on the TiO_2 structure and photocatalytic activity, but as will become clear, many defects do not occur alone but only together with others. Doping is not a topic of this review article but we would like to point out the effect of sodium uptake from the substrate. The defect state of the thin film, as well as its crystal phase, influences its electronic nature. As a result the observed optical band gap and the charge

carrier mobility can be altered, which in turn influences the photocatalytic activity. The latter also depends strongly on the nature and area of the film surface, where the catalytic reaction takes place.

3.1. Crystal structure

An important factor for the photocatalytic activity is the crystal structure of the catalyst. The three most studied polymorphs of TiO_2 are rutile, anatase and brookite, with the former two being the most important for photocatalytic applications. Even though the crystal lattices of rutile and anatase are similar, there are a few significant differences. While rutile has a direct forbidden band gap of 3.02 eV, the one of anatase is indirect allowed and has a value of 3.2 eV. Rutile and anatase also have different numbers of active sites [4]. A common observation is that for anatase always good photocatalytic activity is observed, while rutile shows good photocatalytic activity in some [17] and almost zero activity in other studies [2, 4]. The small difference in band gap between rutile and anatase cannot explain their different activity. A main difference, though, is their recombination rate of photoinduced electrons and holes, which is higher for rutile [2]. Often heat treatment at high temperatures is used to obtain the rutile phase, resulting in the irreversible loss of surface hydroxylation and increased crystal growth, both of which decrease the photocatalytic activity of TiO_2. On the other hand a combination of the two crystal phases can lead to an enhancement of the photocatalytic activity [18-20]. A good example is the P25 powder from Degussa, which has become a reference powder photocatalyst. According to [18, 20] it is the interface between the two phases that yields the active sites.

Brookite has been investigated to a much less extent. A study on single crystal brookite, which had a pale brown color, yielded a band gap of 1.9 eV, which was claimed to be indirect [21]. Since it is difficult to obtain in pure form, not enough is known about brookite to compare its photocatalytic activity to that of anatase and rutile. In [22] brookite powders were synthesized and compared to Degussa P25. As the band gap is substantially lower than that of anatase and rutile it can be expected that its photocatalytic behavior will be quite low.

The relative stability of the three most common TiO_2 modifications is particle size dependent. Below a crystal size of about 15 nm anatase is the most stable phase while for crystal sizes above 35 nm rutile is the stable phase. For the range between 15 and 35 nm rutile and brookite seem to have the same stability [4, 5].

3.2. Crystal defects

Any real material does not have a perfect crystal structure. Even in a single crystal one finds point defects (misplaced lattice atoms/ ions, vacancies,

foreign atoms/ ions) and dislocations. In polycrystalline materials defects are added due to the presence of grain and crystallite boundaries. These defects can introduce energy levels inside the band gap, their location depending on the nature of the defect. According to semiconductor theory [23] donor states are found just below the conduction band, while acceptor states are found just above the valence band. Defect levels deep inside the band gap are *trap levels*, both for electrons as well as for holes. In photocatalysis literature often the term '*trap site*' is used, which denotes a site that can permanently (deep) or temporarily (shallow) bind a charge carrier. The definition of a *trap site* is not straightforward, though, since all levels inside the band gap have the potential to be trap sites. The deeper the trap site lies within the band gap the higher its trapping power, i.e. the lower the chance that the trapped charge carrier can leave the trap within its lifetime. But also the donor and acceptor levels close to the band edges can act as trap sites. The latter enhance the separation of the electron-hole pairs, but if the charge carriers are too strongly bonded they are not available for the photocatalytic redox reaction. As a result, the activity enhancement or reduction by a defect depends strongly on its nature, and the presence of other defects.

3.2.1. Crystallinity

The degree of crystallinity was found to be an important factor influencing the photocatalytic activity of TiO_2. It depends on the actual crystallite size and the ratio between crystalline and amorphous phase present in the material. A higher degree of crystallinity results in a lower number of crystal defects, which is beneficial for the photocatalytic activity of TiO_2. Note that grain size and crystallite size may not be identical. The crystallite size is defined by the domain (within a grain) having the same crystallographic orientation, while a grain is defined by the presence of (visible) grain boundaries. Therefore, it is possible to have different crystallites within one grain.

When trying to asses the effect of crystallite size on the photocatalytic activity one faces as main difficulty how to change the crystallite size while keeping the grain size constant. One needs to increase the temperature to promote crystal growth in anatase TiO_2, which normally results in grain growth and possibly transformation to the rutile structure. Careful studies using SiO_2 as grain growth inhibiting additive have shown that a higher degree of crystallinity results in a higher photocatalytic reactivity [24-26]. The grain growth inhibiting properties of SiO_2 also retard the anatase to rutile transformation which allows annealing at higher temperatures, resulting in improved crystallinity [4]. When decreasing the grain size below ca. 10 to 20 nm the degree of crystallinity is severely reduced due to the high surface to bulk ratio, since the surfaces (grain boundaries) represent a high defect state.

The "*amorphous* TiO_2" phase represents the highest state of disorder, i.e. has a completely random structure [11]. With TiO_2 the definition of amorphous is difficult, as there is always some degree of local ordering observed [10]. Here we will define "*amorphous* TiO_2" as the phase where no signal can be detected by x-ray diffraction (XRD), which means that the material has crystalline domains of a size below the detection limit (< 3-5 nm). Usually grains around 5 nm are detected as very broad peaks around the position expected from the diffraction spectrum of the material and such materials are often labeled '*nanostructured*' [27]. This can be confusing as the usual definition of the nanoscale is < 100 nm [28].

Very little is known on the electronic structure of amorphous TiO_2. Most discussions agree that the high defect concentration should result in poor charge carrier conduction [5, 13]. In [5] it is claimed that for such materials (which they count as nanocrystalline TiO_2) one observes a direct forbidden band gap transition as compared to the indirect allowed transition observed in well crystallized anatase. Completely amorphous TiO_2 is expected not to show any photocatalytic activity [13, 16]. As a result, only rarely the photocatalytic activity of amorphous films or powders is measured [13, 29]. In our own studies we have found that XRD amorphous TiO_2 films can have a substantial photocatalytic activity, though, depending on their microstructure [30]. The photocatalytic activity of such films increases by a factor of almost 3 when crystallizing anatase [30, 31], confirming that a higher degree of crystallinity is indeed beneficial.

3.2.2. Oxygen vacancies (stoichiometry)

Oxygen vacancies represent a special type of defect in TiO_2. They are present when the material is not completely stoichiometric or they can be generated by impurities. As a result, oxygen vacancies will not occur on their own but only in combination with one or more other defects (e.g. Ti^{3+}, impurity). The effect of oxygen vacancies will vary, depending on the exact circumstances of their occurrence. This is reflected in the seemingly contradictory experimental results obtained by different researchers.

Indications that oxygen vacancies are detrimental to the photocatalytic activity were found by [11] and [32] for d.c. magnetron sputtered TiO_2 films. Post oxidation of films using ^{18}O tracer and subsequent SIMS (secondary ion mass spectroscopy) analysis showed that with increasing amount of incorporated tracer the photocatalytic activity decreased [11]. From this, the decrease in photocatalytic activity was attributed to the increase in the number of defects associated with oxygen vacancies in the film. In [32] the photocatalytic activity was linked to the thin film stoichiometry determined by ESCA (electron spectroscopy for chemical analysis) showing a decrease in photocatalytic activity with decreasing oxygen content. In both cases the

conclusion was that for optimum photocatalytic performance the films must be fully stoichiometric.

In [33] preparation of a visible light active photocatalyst of reduced TiO_2 is claimed. The color of the catalyst is reported to be yellow and traces of N were found, indicating doping. In [34-36] it is reported that the doping of TiO_2 thin films or powders with N results in visible (VIS) light photocatalytic activity, which could explain the results obtained in [33]. In a different study by [35] commercially available anatase powder was reduced in a H_2-plasma to have an O/ Ti ratio of 1.68 (ESCA estimate). This powder had a yellowish color and showed a red shift of the optical absorption edge and VIS light photocatalytic activity. An electron spin resonance (ESR) signal of $g = 2.003$ found by the authors was assigned to electrons trapped on an oxygen deficient site [35]. On the other hand, [37] showed that H was incorporated into TiO_2 thin films sputtered in a hydrogen atmosphere. The result was the formation of deep levels inside the band gap. These authors did not investigate the photocatalytic activity of their films, but the results indicate that also in the study presented in [35] the doping with H interferes with the role of the oxygen vacancies.

Density of states (DOS) calculations performed by [11] showed no effect of single oxygen vacancies, but for double oxygen vacancies energy levels inside the band gap were generated. It was suggested that these energy levels can act as recombination centers for the charge carriers, decreasing their concentration and, therefore, the photocatalytic activity of the material. On the other hand, band gap calculations by [38] for anatase showed that oxygen vacancies introduced shallow donor states in he band gap. The authors expect these to increase the photocatalytic activity of TiO_2.

In conclusion, the effect of oxygen vacancies on the photocatalytic activity of TiO_2 is quite complex. The experimental results indicate that the presence of oxygen vacancies alone is not beneficial [11, 32], while a positive effect is found when they occur together with secondary defects due to N or H incorporation [33, 35].

3.2.3. Lattice strain

If the size of a defect is different from its host, a lattice distortion (i.e. strain) is introduced. Some early studies looked at the influence of an applied external stress on the band gap transition of TiO_2 (rutile) [39]. It was found that the band gap increased with increasing applied (uniaxial) stress along the a-axis, yielding a pressure coefficient of dE_g/dP of $-1.19 \cdot 10^{-6}$ eV/ bar (note that the negative sign indicates compressive stress).

In [40] the high band gap of 3.4 eV observed for magnetron sputtered anatase TiO_2 thin films as compared to the bulk value of 3.2 eV was attributed to the distortion of the TiO_2 unit cell. Related authors also performed

experiments and ab-initio calculations [41, 42] to determine the influence of lattice distortions (i.e. lattice strain) on the band gap of rutile and anatase TiO_2. The increase of the band gap with decreasing lattice constant a and increasing lattice constant c was confirmed by experimental results of these authors. From these results one can extract a value of $-4.89 \cdot 10^{-6}$ eV/ bar for the dependence of the band gap E_g on an applied uniaxial stress along the a-axis [15], which is on the order of the one for rutile (see above). This shows a good agreement between the stress measurements and the strain calculations, considering that rutile has a higher Young's modulus than anatase [43].

3.3. Sodium contamination

Early studies discovered that the photocatalytic activities of annealed TiO_2 thin films depended strongly on the type of substrate used [44]. It was suspected that ions diffusing from the substrate into the film during annealing influenced its activity. Other authors investigated the effect of a soda-lime glass substrate on the photocatalytic activity of heat treated TiO_2 films [12, 46].

In [12] the resulting decrease in photocatalytic activity was related to the effect of Na^+ on the grain growth in the thin film upon heat treatment. Na^+ was found to retard the crystallization of anatase while increasing the particle size in the film. The photocatalytic activity was correlated to the particle size of the films, rather than to their Na^+ content, the photocatalytic activity increasing with decreasing particle size (in the range of 25 to 40 nm). Na^+ was expected to form a shallow donor state in TiO_2, which would make it a rather unlikely recombination center. Therefore, the authors conclude that Na^+ in the films influences the photocatalytic activity by changing the particle size and not by acting as recombination center.

Experiments in our group have shown that Na^+ inhibits crystallization by decreasing the degree of crystallinity and increasing the temperature needed for crystallization [46]. The photocatalytic activity was not only decreased for crystalline films, but also for films annealed below the crystallization temperature, which remained amorphous and in all cases the grain size remained constant [31, 46]. Latter indicates, in contrast to [12], that it is indeed the uptake of Na^+ into the films that degrades the photocatalytic activity. In [45] the diffusion of Na^+ into the TiO_2 thin film from soda-lime glass was measured by ESCA depth profiling and a direct link between its lower photocatalytic activity and the Na^+-concentration was made. It was suggested that Na^+ acted as recombination center for electrons and holes.

Independent of the exact cause, the uptake of Na^+ decreases the photocatalytic activity of TiO_2 thin films substantially. As a result most investigators use soda-lime free substrates or a SiO_2 barrier coating [11, 47] to

avoid incorporation of Na^+ when a heat treatment step is needed after deposition. Uptake of Si from any kind of glass is observed, but this is not reported to have a negative influence on the photocatalytic activity of TiO_2 thin films [45]. In conclusion, the best strategy concerning the effect of Na^+ on the properties of TiO_2 is to avoid the possibility of Na^+-contamination by the correct choice of (glass) substrate.

3.4. Surface hydroxylation

The surface hydroxyl groups are important shallow trap sites for the holes generated upon UV-illumination in TiO_2 (section 2.1). Therefore, they play a crucial role in the photocatalytic process. The degree of surface hydroxylation not only depends on the relative humidity but also on the surface structure of the catalyst. Hydroxyl groups are formed by water dissociation, so that it is favorable to have paired acid/ base sites situated at the appropriate distance [4]. The water molecules are initially bonded to the surface sites with an acid character, namely Ti-cations with a coordination number lower than the bulk value of 6. Adjacent surface sites with a basic character, namely bridging oxygen atoms, then accept the proton. The conclusion is that the degree of surface hydroxylation increases with the number of acid sites present at the surface. The coordination number of Ti at the surface depends on the terminating crystal facet [6] but also decreases with its oxidation state. Therefore, sub-stoichiometric surfaces show an increased surface hydroxylation [4]. Si also has a lower coordination number of 4 (bulk) and it is reported that its addition to TiO_2 increases the degree of surface hydroxylation [48]. Consequently, the catalyst preparation conditions play a major role in surface hydroxylation [4, 49]. The degree of surface hydroxylation in a gas atmosphere is related to its water content, while in solution it is related to its pH. Therefore both factors have an influence on the photocatalytic reaction rate [4].

3.5. Particle size

In general, particles in the nanometer range (< 100 nm) show a physical and chemical behavior different from larger sized material. For very small particles (< 35 nm) their size has an effect on the crystallographic phase stability and the chemical activity (section 3.1). It has become common to call such materials *nanostructured*, with *nanoparticles* being ultrafinely dispersed particles and *nanocrystalline materials* being materials with a fine crystallite or grain size. Unfortunately the terms 'crystal' and 'grain' are sometimes used as synonyms even though they describe something completely different (section 3.2.1).

Regarding the photocatalytic activity of nanocrystalline TiO_2 there is quite some discussion on the influence of the crystallite and particle size. The degree

of crystallization (i.e. the ratio between crystalline and amorphous phase) will decrease with decreasing grain size due to the increasing influence of the (amorphous) grain boundaries. Often the grain size and/ or crystallinity of the thin films are not clearly defined or have a large spread, so that dependencies cannot be defined well.

In the following we highlight the most important effects that are associated with a nanoscale structure in TiO_2. So far, no solid proof could be provided that the general photocatalytic efficiency of very finely grained (< 10 nm) TiO_2 (significantly) exceeds that of larger grained material, as long as the grain size remains below 100 nm. The photocatalytic activity of TiO_2 having a (lateral) grain diameter above 1 μm has been studied little.

3.5.1. Chemical activity

With nanostructured materials the particle surface area is large compared to the bulk of the particle. As a result the surface energy becomes more dominant, changing the Gibbs free energy of the material and, therefore, its chemical activity. On the other hand, the large surface area itself increases the catalytic activity of the nanostructured material by offering more active sites for the reaction to take place. The surface presents a defect state due to the presence of dangling bonds on the TiO_2 surface, which is sometimes interpreted as an increased number of oxygen vacancies. It is argued that this is why nanosized TiO_2 will also have a higher density of oxygen vacancies than large grain size TiO_2 [5]. These defect states are preferred sites for the adsorption of water and O_2 from the ambient air, the former resulting in the formation of hydroxyl groups (section 3.4).

3.5.2. Optical and electronic properties

The fact that the grain dimension is smaller than the wavelength of visible light (ca. 400-700 nm) also results in different interaction with such light. Compared to films with a larger grain size, which can be opaque, one observes that the degree of light scattering is decreased [8, 50]. This means that the films remain optically transparent. The small grain size also has the advantage that the charge carriers do not have to migrate far before they reach the surface of the grain, where they are needed for the redox reaction at the catalyst surface (Figure 1).

On the other hand, the small particle size is associated with a higher number of defects in the form of surfaces [4], while the number of inner grain defects is decreased [51]. Defects act as trap sites, so that the number of trap sites decreases in the bulk but due to the increased surface area a larger number of surface trap sites is generated. When the ratio of surface to bulk reaches a critical value the increasing number of trap sites can offset the positive influence of the short carrier migration distance. As a result, there is a critical

size below which the surface recombination of electrons and holes becomes dominant due to the increased surface to volume ratio. The optimum grain size is reported to be around 10-20 nm [52], below which a decrease in photocatalytic activity is observed.

3.5.3. Quantum size effect (very small grain sizes)

For decreasing particle sizes, quantum mechanical calculations show a transition from semiconductor to molecular properties. This means that the band structure of the semiconductor breaks up into quantum levels, the transition point being where the particle size reaches the order of the de Broglie wavelength of the charge carriers in the semiconductor. For most semiconductors this lies in the range of 5-25 nm, the exact value depending on the material [8]. This change in electronic structure is commonly referred to as '*Quantum size effect*' (QSE) or '*Q-effect*' and the respective particles are called '*Q-particles*'. The most wide-spread, simple theoretical framework to study the influence of confinement effects and how they depend on the primary particle size is the so-called effective mass approximation (EMA). More comprehensive discussions of the quantum size effect and the EMA are given in [2, 5, 7, 8, 53, 54]; the original theoretical framework was developed by Brus in his work on CdS clusters [55].

Strictly speaking the theory behind the quantum size effect is only valid for (i) freely suspended particles, where the charge carriers are confined within the particle and (ii) a covalent material, where the electronic band theory is valid [55]. Both conditions are not fulfilled in the case of a TiO_2 thin film, where the bonding is partially ionic and the particles are embedded, allowing charge carrier migration across the grain boundaries. Latter is also valid for strongly agglomerated powders where charge carrier transport is no longer limited to the individual grains but to the (much) larger agglomerate. The quantum size effect could not be verified for (anatase) TiO_2 [5, 7, 55], even though claims have been made that it is responsible for the blue shift of the band gap in nanocrystalline anatase powder [54].

3.5.4. Nature of the band gap transition

There is some discussion in literature about the nature of the band gap transition in nanostructured (anatase) and amorphous TiO_2. Some authors [5, 54] claim that for small grain sizes the band gap transition switches from indirect to direct, which is of interest as the absorption at threshold and the emission of light is much stronger for the direct transition. This should result in a more efficient absorption of light and in improving the photochemical performances of the nanostructured materials.

In [54] it was decided on basis of the best fitting results to the experimental data that the band gap of very finely grained anatase was direct.

The authors suggest that photoluminescence studies could be used to support the observations. In [5] it is argued that the confinement of charge carriers to a limited space causes their wave functions to spread out in momentum space, in turn increasing the likelihood of radiative transitions for bulk indirect semiconductors. Again, this argument is not valid for thin films and agglomerated powders where the charge carriers cannot be strongly confined (3.5.3). In [52] the enhancement of absorption observed in small nanocrystals is claimed to be the result of the very high surface to volume ratio. Here the share of surface atoms is sufficiently high to increase the chance of surface absorption, which increases the light absorption in total. Both arguments are actually based on the fact that a direct transition shows a stronger light absorption than an indirect transition.

3.6. Microstructure (film surface area)

There are few consistent studies which investigate the effect of the thin film microstructure on the photocatalytic activity. Mostly the film crystallinity is studied but the grain structure and porosity are generally ignored. This is surprising because especially the film porosity will influence the active surface area, which in turn has a strong effect on the photocatalytic activity. Our own studies showed that the film microstructure is strongly related to the photocatalytic activity of the TiO_2 thin films [30, 31].

It is usually impossible to determine the BET (Brunauer-Emmet-Teller absorption isotherm) surface area of a thin film because the total surface area of the sample is too small for the standard BET analyzers. These have a detection limit for the total surface area in the order of 0.1-1 m^2 and receptacle sizes in the cm^3 range. Additionally the receptacles are designed to analyze powder samples, so that coated substrates have to be cut into pieces, which results in a high amount of uncoated surface being tested. Note that the surface area of a (powder) catalyst is usually reported in m^2/g, which is not applicable for a thin film catalyst where the weight of the thin film is normally more than 3 orders of magnitude lower than that of the substrate. One method to estimate the active surface area of a thin film is by looking at its microstructure. Pores will add to the surface area of a thin film (section 3.6.2), but their size will determine whether they can add to the active surface area (section 3.6.3).

3.6.1. Determination of the thin film porosity

A simple way to estimate the porosity is through the refractive index of the thin film, which can easily be determined from ellipsometric or optical transmission measurements [56, 57]. The refractive index of a mixed compound can be calculated from the indices of the individual components, using e.g. the Lorenz-Lorentz equation [56]:

$$\frac{n^2-1}{n^2+2}\frac{M}{\rho}=\sum_{i=1}^{m}\left(\frac{n_i^2-1}{n_i^2+2}\frac{f_i M_i}{\rho_i}\right) \quad \text{with} \quad \sum_{i=1}^{m} f_i=1 \tag{3}$$

where n is the refractive index of a composite material of average molecular weight M and density ρ which can be viewed as consisting of m materials each having the mole fraction f_i, the molecular weight M_i and the density ρ_i.

A porous material can be modeled as a mixture with air. Since the refractive index of air is close to 1, equation (3) simplifies to:

$$1-P=\frac{n^2-1}{n_i^2-1}\frac{n_i^2+2}{n^2+2} \tag{4}$$

with P denoting the porosity, defined as

$$P=1-f_i\left(\frac{M_i}{\rho_i}\frac{\rho}{M}\right) \tag{5}$$

Expression (5) allows calculation of the film porosity from the refractive index if there are no other influences like second phases or dopants. Nevertheless, any calculation of the porosity should be taken as an estimate only.

3.6.2. Estimate of the surface area of a thin film from its porosity

When depositing a thin film by d.c. magnetron sputtering under the conditions that yield porous zone 1 growth (please refer to section 5.2) one obtains irregular and separated column-grains (Figure 2).

These column-grains have rounded tops and an elongated, approximately cylindrical shape. The rounded tops will in all cases increase the surface available for catalysis. The side surfaces of the column-grains can only participate

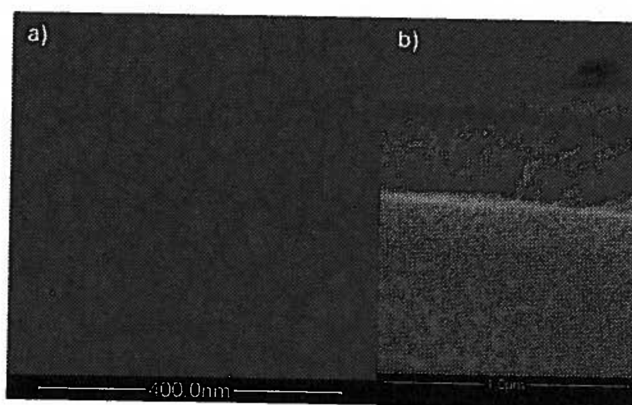

Figure 2. Scanning electron microscope (SEM) images of TiO_2 thin films deposited in zone 1 structure by d.c. magnetron sputtering (60 W, 1.4 Pa, TiO_{2-x} ceramic target): a) top view, b) cross section.

when the inter-grain spacing is large enough to allow diffusion of the reactant and reaction products. This inter-grain spacing actually defines the pore size in the thin film. In the following we shall first calculate the increase in the thin film surface area due the microstructure and then estimate the pore size for a given grain size, film thickness and density.

If a thin film has a completely dense structure and a flat surface, the active surface area is equal to the geometrical area of the substrate (Figure 3., left). A rough surface, on the other hand, will have a larger area. We can estimate this increase by assuming that the surface consists of a collection of semi-spheres (the tops of the individual grains, see Figure 3., right). A circle with radius R will have a flat surface area of πR^2, but a semi-spherical surface area of $2\pi R^2$. As a result, the gain in surface area when going from a flat to a rough surface, consisting of half spheres, is only a factor of 2.

Much more effective area can be gained if the film consists of free-standing columns (Figure 3., right). For the sake of simplicity we assume that every column has a flat top and a fixed square column section, with size d (Figure 4). The height of the columns is identical to the film thickness h. Porosity is taken into account by separating the columns by a distance f (Figure 4).

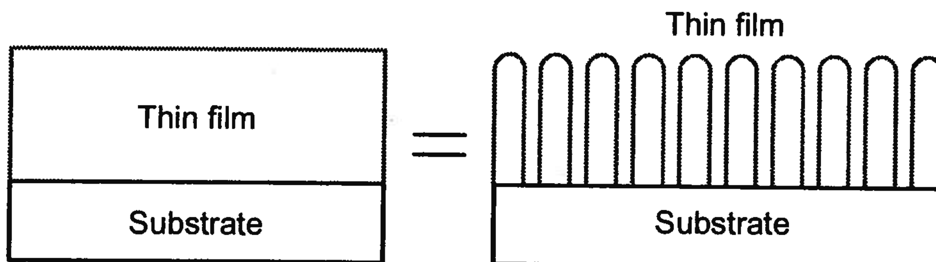

Figure 3. Sketch of a thin film (in cross section) consisting of (spaced) column-grains (right), illustrating that the dense structure normally assigned to a thin film (left) is not necessarily correct.

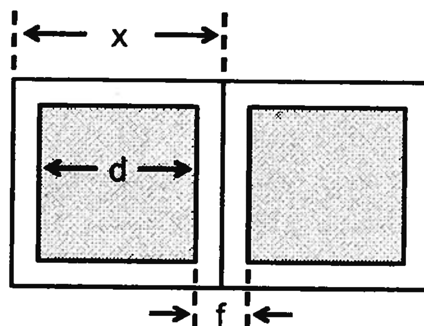

Figure 4. Sketch of the column-grain thin film structure (top view) showing the cell used for calculation of the surface area and the free space between the column-grains.

The projected (geometrical) surface area, equal to the substrate area (which is assumed flat) is $(d+f)^2$ per grain. On the other hand, the total column surface area, including the column sides, is:

$$d^2 + 4dh \quad (6)$$

The ratio of the active surface area of the free-standing columns to the area of a dense film will be:

$$\frac{d^2 + 4dh}{(d+f)^2} \approx \frac{d^2 + 4dh}{d^2} \quad (7)$$

since $f \ll d$ (see Table 1.) for realistic thin films.

If we take a film thickness of $h = 400$ nm and a column diameter of $d = 50$ nm, this ratio is 33, so that the total active area increases considerably when the film consists of free-standing columns.

3.6.3. Estimate of the pore size of a thin film from its porosity

The porosity P can be defined as the fraction of free space in the film, and is a value which can be estimated from the effective refractive index of the films according to equation (4). If the columns themselves are completely dense, then we can relate the porosity P to the spacing f between the column-grains (Figure 4.):

$$P = \frac{(d+f)^2 - d^2}{(d+f)^2} \quad (8)$$

Solving for f yields:

$$f = d\left(\frac{1}{\sqrt{(1-P)}} - 1\right) \quad (9)$$

The calculated spacing f between two column-grains for a given porosity P is listed in Table 1. Note that these values only give an estimate since they were calculated taking the column-grains as 100% dense. Since this is most likely not the case the true inter-column spacing will be smaller.

The inter-grain spacing f is nothing other than the pore size of the thin film. According to the IUPAC (International Union of Pure and Applied Chemistry) definition one distinguishes the following different pore types according to their diameter x [58]:

macropores: $x > 50$ nm
mesopores: $2 \leq x \leq 50$ nm
micropores: $x < 2$ nm

Table 1. Calculation of the inter-grain spacing f from the porosity according to Figure 4.

Porosity P (%)	1.0	2.5	5.0	7.5	10.0	12.5	15.0	17.5	20.0	22.5	25.0
Inter-grain spacing f (nm)	0.25	0.64	1.3	2.0	2.7	3.5	4.2	5.1	5.9	6.8	7.7

From Table 1. one can see that from a porosity of about 7.5% on the thin films are mesoporous. Usually micropores are too small to be catalytically active, while mesopores are known to increase the active surface area of a catalyst. The minimum size a pore needs to have in order to be active depends on several factors. These include the diffusion coefficient of the reactants into and products out of the pores (determined by their size and electronic nature), their concentration in the atmosphere surrounding the catalyst and the flow rate of the carrier gas stream passing over the catalyst bed.

Our own results have shown a strong dependence of the photocatalytic activity of column-grained TiO_2 thin films on porosity values up to 22.5%, when measuring the breakdown of ethanol in a batch reactor [59]. Increasing the porosity above this value no longer had an influence on the photocatalytic activity, indicating that a critical pore size was reached which allowed the breakdown reaction of ethanol to proceed freely.

3.7. Film thickness

Not much is reported on the effect of thickness on the photocatalytic activity of thin films [12, 45, 60], even though some authors are aware of the influence and correct for the variations in sample thickness [13]. In order to study the true influence of film thickness it is important that the structure of the film does not change with film thickness, which was not the case in [60]. In [45] thin films with thickness between 50 and 250 nm were studied. Here it was found that the photocatalytic activity reached its maximum at ca. 140 nm, after which it remained constant. In [12] a critical film thickness of ca. 360-430 nm is reported. The difference between the two studies indicates that this critical film thickness is dependent on the thin film preparation techniques and/ or the experimental setup for testing their photocatalytic activity. As we have shown in section 3.6.3 the density of a column-grained structure determines its inter-grain porosity, and as a result its surface area. The catalytic activity of these pores will depend on the experimental setup, including the size and nature of the organic test substance used. Neither [12] nor [45] report anything on the microstructure of the thin films studied.

Tada et al. tried to determine the nature of this critical film thickness and proposed that there is a limited diffusion length of the charge carriers and a

cumulative light absorption with increasing film thickness [45], as depicted in Figure 5. Their experimental results indicated that the critical film thickness was ca. 100-150 nm, from which they deduced a charge carrier diffusion length of about 300 nm.

Our own experiments using porous TiO_2 thin films (22.5% porosity) with a column-grain structure have confirmed this reasoning. The data showing the dependence of the photocatalytic activity on the film thickness (Figure 6.) can be fitted at first sight by two linear graphs (dark). On the other hand, an exponential fit describing the light absorption in the film (at an intermediate wavelength of the given lamp spectrum) can also be applied (light, dotted curve).

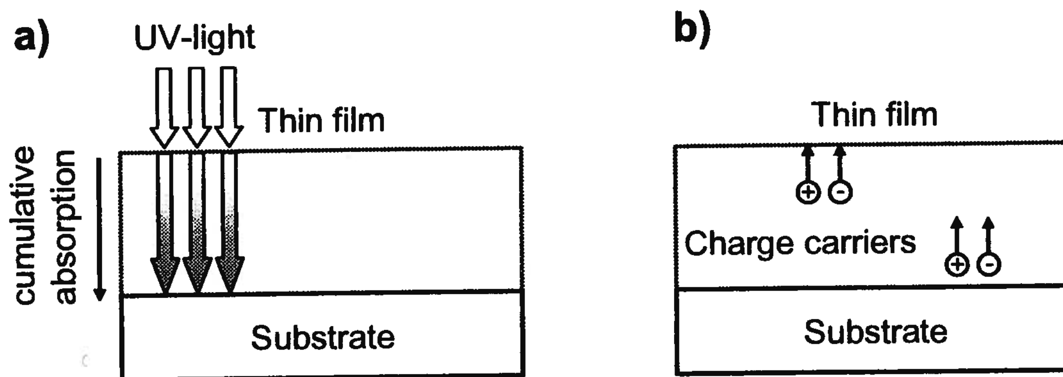

Figure 5. Sketch showing the limiting factors for the photocatalytic activity of thin films: (a) increasing light absorption, (b) the charge carrier diffusion length.

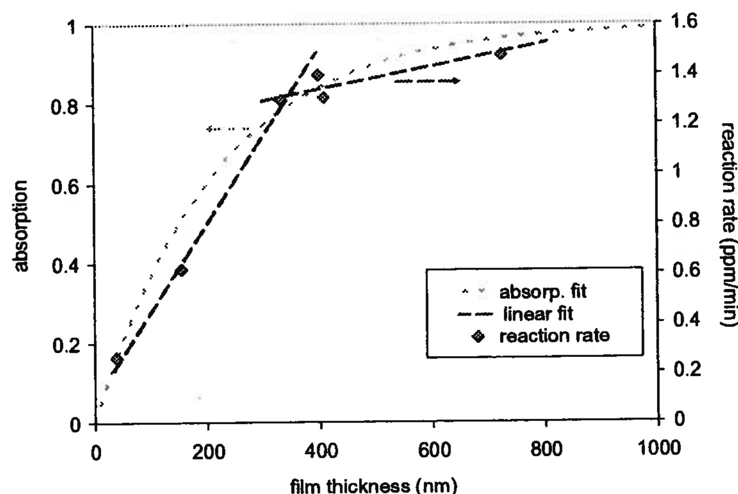

Figure 6. Dependence of the photocatalytic activity on the film thickness for XRD amorphous TiO_2 thin films deposited by d.c. magnetron sputtering (TiO_{2-x} ceramic target, pure Ar at 1.4 Pa, 60 W). The data are fitted by two linear sections which seem to indicate a possible critical film thickness of about 350 nm, and an exponential fit describing the absorption of UV-light with increasing film thickness.

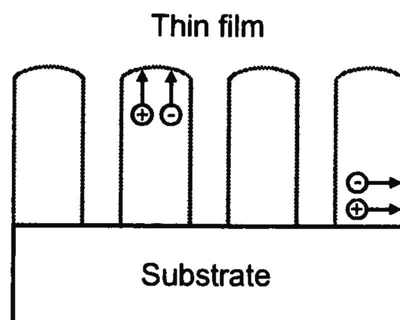

Figure 7. Sketch showing the possible diffusion paths of photogenerated charge carriers in column-grained TiO_2 thin films.

In order to determine which of the two mechanisms is correct we performed separate photocatalytic measurements for two samples of different thickness using (i) the complete spectral range of the lamp and (ii) only the wavelengths above 345 nm. The results indicated that the higher wavelength light, which enters deeper into the thin film, showed a similar photocatalytic activity per active photon arriving at the film surface. This should not be observed if the diffusion length of the charge carriers was the limiting factor.

Additionally the column-grained film structure (Figure 3.) also explains, why the carrier diffusion cannot be the limiting factor for these porous films. In Figure 7. possible diffusion paths of the charge carriers in the column-grains are shown. Since the diameter of the columns is only about 50 nm, charge carriers generated anywhere inside the grain do not need to diffuse more than about 25 nm to reach its surface. As a result, the limiting factor that the thickness imposes on the photocatalytic activity is the fact that most of the incoming light is absorbed in the first few 100 nm of the film. Increasing the film thickness does not lead to much more absorption. This allows to use the linear expressions from Figure 6. to determine a '*critical value*', above which the photocatalytic activity depends less strongly on the film thickness.

The conclusion is that the film thickness is an important parameter for the photocatalytic activity of TiO_2 thin films. Care must be taken when designing experiments to find the critical film thickness above which the photocatalytic activity is less dependent on this factor to avoid experimental errors. As already discussed, the active pore size depends on the chosen organic test substance, which can be expected to influence this critical film thickness.

3.8. Designing a highly photoactive TiO_2 thin film: Summary

To summarize sections 3.1 to 3.7, we can state that to optimize the photocatalytic activity of a TiO_2 thin film one has to control two parameters, namely the surface area and the defect structure, which is primarily reflected in its crystallinity.

- The surface area of the thin film can be increased by decreasing the grain size and increasing the porosity. Important for finding the minimum pore size will be the dimensions and the nature of the organic substance to be broken down.
- The crystallinity of the thin film increases by increasing the number of crystallites as well as their size. Since the grain surface can be taken as a highly defective, non-crystalline phase the crystallinity increases with grain size (lower surface to volume ratio).

The result is that one needs to balance grain size (high surface area) and crystallinity (low defect state) for the optimum results. In general it is interesting to keep the number of defects as low as possible.

Additionally, it is necessary to avoid contamination of the TiO_2 thin film by inward diffusion of Na or other ions from the substrate.

4. Ceramic thin film deposition techniques

4.1. General considerations

The variety of thin film deposition techniques used for TiO_2 can roughly be divided into two areas, namely wet chemical and vapor deposition. The former is a solution based technique where the substrate is either coated with a colloidal solution (sol-gel) or a TiO_2 thin film is grown onto the substrate (electrochemical deposition). In vapor deposition various techniques are employed to generate a vapor phase of Ti, some precursor or TiO_2. In the former two cases the TiO_2 film is formed by oxidation at the substrate.

An important issue is also the choice of substrate material. It must be compatible with the deposition conditions as to remain inert and undamaged during deposition. The substrate must also be resistant to the temperatures required for calcination/ crystallization of the thin film and not cause any contamination (see section 3.3). An important example are polymer substrates which have a rather low temperature resistance (typically 150°C), and can pose a problem in vacuum chambers due to out-gassing of e.g. water.

4.2. Wet chemical techniques

The most important wet chemical techniques employed for thin film deposition are sol-gel and electrochemical deposition, with the former being by far the most frequently used [4, 11]. We will briefly discuss the main aspects of these two techniques and refer to the more extended literature for further reading.

4.2.1. Sol-gel

The sol-gel technique has some profound advantages for thin film deposition, namely purity, homogeneity, flexibility and ease of processing.

Depending on the type of precursor used, one distinguishes between the non-alkoxide and the alkoxide route. Former uses inorganic Ti-salts, while latter uses metal-organic (alkoxides) as precursors. The first step in the sol-gel process is the formation of a colloidal suspension of solvent stabilized titanium oxide particles (sol) by controlled precipitation. The sol is then coated onto the substrate by different techniques like dip or spin coating. During drying (evaporation of the solvent) a gel is formed, which has a very loose structure. Any remaining inorganic salt must be carefully removed by washing of the gel film.

The route employed most is the one using alkoxides (generic formula O-R, with R denoting an organic rest). The most popular ones are the tetra-ethoxide, iso-propoxide and n-butoxide of Ti, with the general formula $Ti(O\text{-}R)_4$. Here the sol is formed by controlled hydrolysis followed by poly-condensation of the metal-organic precursor. In order to have good control of the process one aims to use precursors that allow for separating and slowing down the two steps.

For both routes the structure of the thin film can be influenced by the nature of the precursor and the solvent as well as by adding surfactants. Since the film thickness achieved by one coating cycle is below 100 nm, several coating cycles are needed to obtain thicker films. A very good overview on depositing sol-gel films of TiO_2 can be found in [4].

In earlier years the limitation of the sol-gel process was the necessity to calcine the films at temperatures between 500-600°C, in order to achieve good stoichiometry and crystallinity [12] which limited the applicable substrate materials. More recent investigations showed that the need for such high temperatures was due to the wrong substrate choice and caused by Na-contamination of the films (section 3.3). For good bonding of a sol-gel film with a glass substrate temperatures above 400°C are still necessary, though [4].

4.2.2. Electrochemical deposition

Electrochemical deposition, also referred to as *electrolysis* or *electroplating*, is a technique which has been known for a long time. Here the TiO_2 thin film is deposited onto a metal electrode from a solution of a Ti-compound like $TiCl_4$ [61, 62], $TiCl_3$ [62, 63], $Ti(SO_4)_2$ [64-66] or $(NH4)_2[TiO(C_2O_4)_2]$ [67]. Care must be taken that the chosen salt does not hydrolyze in the solvent used, which would result in precipitation (i.e. powder formation). Often hydrogen peroxide is added as oxidant in combination with the Ti-compound [61, 64, 66]. Surfactants can be added to influence the growth and structure of the deposited film [62, 68]. If the substrate is conductive a d.c. process can be used [62, 64]. As the deposited coating is insulating, often a pulsed d.c. [32] or a.c. [67] process is necessary. The latter two also have the advantage that they can be used for coating an insulating

substrate or to fill the porous structure of an alumina film grown by anodic oxidation [32, 67].

In most cases a porous, XRD amorphous TiO_2 film is deposited, which is beneficial for catalytic applications. Annealing at temperatures between 300 and 500°C is needed to obtain crystalline anatase films [61, 66, 69]. Some references report direct deposition of crystalline TiO_2 [62].

A related technique is the anodic oxidation of Ti-metal, where a thin oxide film is grown on the surface of the anode. There are few reports about growing such films for photocatalytic applications [70].

4.3. Vapor deposition techniques

Vapor deposition techniques include chemical vapor deposition (with or without plasma enhancement, i.e. CVD or PECVD) and physical vapor deposition (PVD), including electron beam evaporation and (magnetron) sputtering. With (PE)CVD powders as well as thin films can be deposited, depending on the processing conditions. Physical vapor deposition techniques are used exclusively for thin film deposition. The main advantage of vapor deposition techniques, especially PVD is that good adhesion of the film to the substrate can be achieved. A second advantage of vapor deposition techniques is that the process conditions can be controlled to yield crystalline thin films without external substrate heating, while substrate self heating can occur during the process.

4.3.1. Chemical vapor deposition techniques

Chemical vapor deposition (CVD)

Chemical vapor deposition (CVD) techniques are based on the oxidative decomposition of a volatile Ti-precursor to form a TiO_2 film on the substrate (Figure 8.). Variations of the technique include using an aerosol, which is formed in the reaction chamber, so that droplets are deposited. If a thin film is desired, care has to be given, that the process does not result in powder formation.

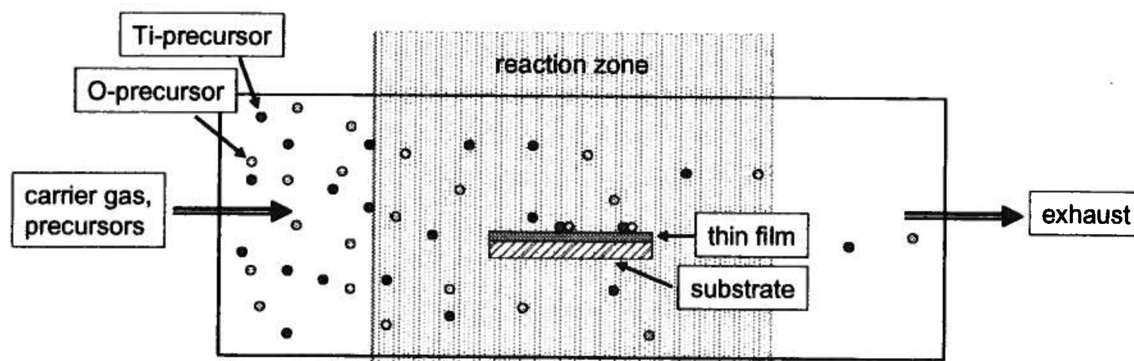

Figure 8. Scheme of a generic chemical vapor deposition process.

A study showing the factors determining powder or film formation is given in [71]. In order to promote the deposition of a well adhering, crystalline film it is necessary to work at elevated temperatures or use other methods to introduce additional energy into the reactive zone. The main advantages of CVD are that complex surfaces can be coated and the film porosity can easily be controlled.

In the original (CVD) process a volatile inorganic Ti-compound ($TiCl_4$) is decomposed at the substrate in the presence of oxygen and/ or water to TiO_2 and HCl. The Ti-precursor is introduced into the reactor together with a carrier gas, usually by bubbling it through the precursor fluid. Initially thermal energy (heat) was used to promote the oxidation reaction and enhance film crystallization. At temperatures between 300 to 700°C the anatase phase is formed while at higher temperatures the rutile phase crystallizes. The exact crystallization temperature depends on the nature of the process. Further development of the CVD technique implemented other energy sources which allow thin film crystallization at lower temperatures. Additionally, the carrier gas flow and the concentration of the reactants influence the structure and properties of the deposited film. Depending on the technique and the reaction parameters used, quite high deposition speeds up to 10 nm/s can be reached. In the following some variations of the standard thermal CVD technique will be discussed briefly.

Since $TiCl_4$ is a quite unstable compound, investigators started using organic Ti-compounds, i.e. *metal-organic* (MO) precursors, which has led to the term MOCVD. The standard organic precursor is titanium tetra-isopropoxide (TTIP), also called Ti(IV)-isopropoxide, with the chemical formula $Ti(O\text{-}CH(CH_3)_2)_4$, which is normally implemented in form of a solution in isopropanol. This material has a quite good stability towards ambient air and a low toxicity so that it is easy to handle. Other organic Ti-compounds have also been used [72-75], including precursors that do not need addition of oxygen or water [76]. There is a continuous development of new precursors with the aim to influence the deposition process and, as a result, the film properties.

To enhance the dissociation of the precursors and or lower the reaction temperature different secondary energy sources can be used. Examples are (r.f.) plasma enhancement (PECVD) [77-87], thermal plasma (TPCVD) [88], laser irradiation (LCVD) [89, 90] or ultraviolet light (UV) [91], with plasma enhancement being the most implemented one.

Methods different than bubbling can also be used to introduce the Ti-precursor(s), e.g. liquid injection (LICVD) [91, 92], liquid delivery [93], liquid mist spray [72] or liquid aerosol [94]. Related to the latter two techniques is spray pyrolysis. The pressure in the reaction chamber can range from atmospheric (APCVD) [71, 72, 95, 96] over low pressure [60, 84, 85] to high vacuum [25].

Atomic layer deposition

Further development of (MO)CVD has led to ALD (atomic layer deposition) [97-101]. Here the reaction conditions and precursors are chosen in a way as to yield a layer-by-layer growth of the film: First the Ti-precursor is introduced and coated as a monolayer on the substrate, then an oxidizing agent is introduced (e.g. O_2), which oxidizes this layer. By repeating these steps a (dense) thin film can be grown. Due to the low deposition rate, being on the order of 10^{-3} nm/s, ALD is a very slow and therefore very expensive deposition technique. The advantage is, though, that any surface shape can be coated in a very homogeneous manner, leading to so-called conformal coatings.

4.3.2. Physical vapor deposition techniques

Evaporation

Most evaporation techniques used for the deposition of TiO_2 thin films are derived from electron beam evaporation (Figure 9.). Here the source material, usually TiO_2, a sub-oxide [102, 103] or Ti-metal [104] is heated with an intense electron beam under an oxygen partial pressure below 0.1 Pa. The addition of oxygen is needed to obtain stoichiometric films. In a standard setup a low chamber pressure is needed to prevent scattering of the evaporated particles and oxidation of the electron gun. If the electron gun is differentially pumped higher pressures can be used in the deposition chamber. The evaporation rates can be quite high, namely on the order of 10 nm/s. Crystalline (anatase or rutile) thin films can be obtained by either heating the substrate during deposition or annealing after deposition. The microstructure of the thin films can be controlled by the starting materials, the substrate temperature [105, 106], the deposition (O_2) pressure [107, 108], the evaporation rate and the angle of incidence [104]. Studies looking at a variety of parameters are given in [102, 109]. An additional plasma [106] or ion (beam) source [102, 105, 109, 110] can be implemented to control the thin film microstructure and stoichiometry.

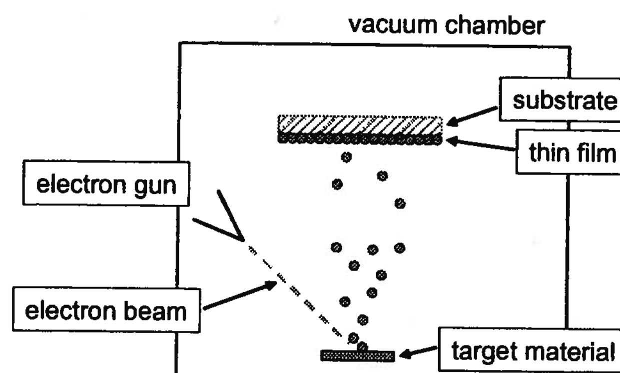

Figure 9. Scheme of a setup for electron beam evaporation.

Molecular beam epitaxy

Molecular beam epitaxy (MBE) is a very precise evaporation technique using an ultra low deposition speed. Here the Ti-precursor and the oxidizing agent are introduced together as atomic or molecular beams. The layers are grown on a substrate which has a good lattice matching with the TiO_2 phase to be grown, so that the thin film follows the crystallographic orientation of the substrate surface (epitaxial growth). In order to achieve this type of growth the deposition rate has to be rather low and the substrate needs to be chosen as to yield a lattice match with the desired crystallographic orientation and phase of TiO_2. A very good review on the subject of MBE growth of oxide thin films, including rutile and anatase TiO_2 is given in [111]. Since MBE requires single crystalline substrates, this is a technique which is not likely to be implemented for large scale deposition of photocatalytic layers. Nevertheless, it is an interesting technique for studying specific crystal planes of TiO_2.

Sputtering

In diode sputtering a discharge is generated by applying a d.c. voltage between two electrodes (anode and cathode) in a low pressure gas, typically argon (Figure 10, left). The ions generated in the discharge are accelerated towards the cathode (target), bombarding its surface, which results in the removal (sputtering) of cathode atoms [112, 113]. The sputter rate from a diode discharge is low (partially due to the rather high pressures of 1-10 Pa needed to sustain the discharge).

An improvement is the use of a magnetic field confinement of the discharge above the cathode, i.e. magnetron sputtering [114, 115] (Figure 10, right). This technique allows deposition at lower gas pressures (0.1 to 1.0 Pa) and as a result, higher deposition rates. Further modifications are the use of r.f and pulsed d.c. or a.c. power to avoid charging effects when sputtering from an insulating target or in the presence of a reactive gas which forms a non-conductive

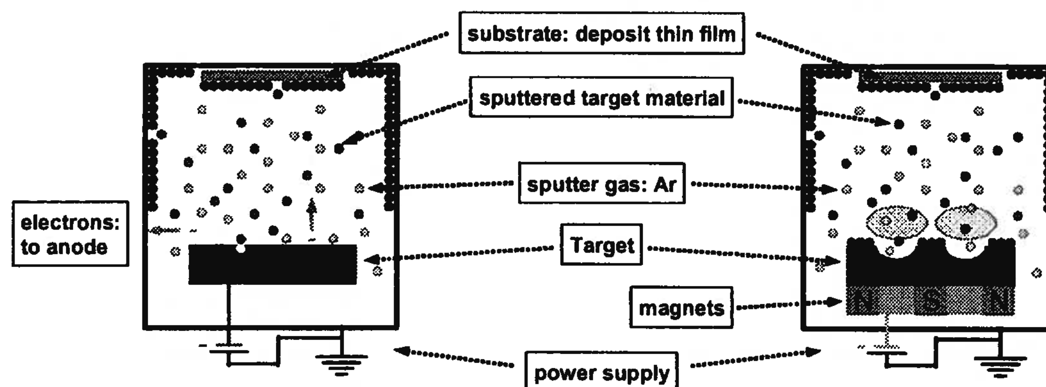

Figure 10. Scheme of d.c. diode (left) and magnetron (right) sputtering.

compound with the sputtered target material. The deposition of TiO_2 thin films with (reactive) d.c. magnetron sputtering will be discussed in more detail in section 5.

5. Deposition of TiO_2 thin films by reactive d.c. magnetron sputtering

In this chapter we will first give an overview of how the technique of (reactive) d.c. magnetron sputtering can be used to deposit TiO_2 thin films (section 5.1). We will then discuss the parameters controlling thin film growth with this technique (section 5.2) and how they can be implemented for growing TiO_2 thin films having different crystal and microstructures (section 5.3).

5.1. Reactive d.c. magnetron sputtering

D.c. magnetron sputtering is a physical vapor deposition technique, which is operated in a vacuum system at total gas pressures of 0.1-1.0Pa. If the sputtering gas is inert, it will not undergo any chemical reaction with the target material so that the composition of the thin film is controlled by the target composition. When a second gas, which can react with the target material, is added, to the sputtering gas the technique is called 'reactive sputtering' [116-118].

The addition of a reactive gas has profound implications on the sputtering process and, therefore, on the deposition of the thin film. At low reactive gas concentrations the same deposition conditions as for metallic sputtering (inert gas only) are observed, so that metal rich thin films are deposited. For intermediate reactive gas concentrations the process becomes unstable, so that controlled thin film deposition in this range is not possible. For high reactive gas concentrations the discharge conditions are quite different so that one speaks about '*reactive*' sputtering. In this regime a stoichiometric compound

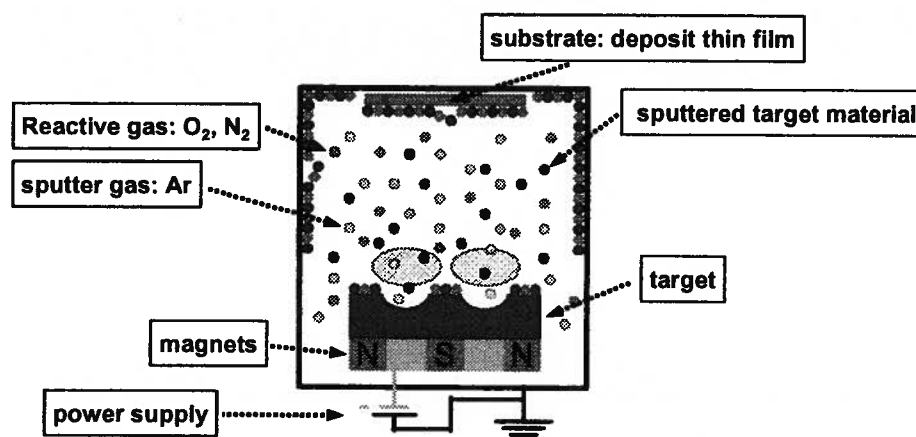

Figure 11. Scheme of a reactive d.c. magnetron sputtering setup.

film is deposited. For reactive sputtering the deposition rate is low, which is unattractive for most applications. Therefore, methods have been developed to stabilize the sputter process for intermediate reactive gas concentration which allows depositing stoichiometric thin films at a higher rate [116-118].

In the case of TiO_2 thin film deposition it is possible to use a sub-stoichiometric ceramic TiO_{2-x} target having a sufficient d.c. conductivity to enable d.c. sputtering [22, 119-122]. In [123] the deposition rate of a $TiO_{1.75}$ target in pure Ar is 50% of the metallic deposition rate and 3 times that of the reactive rate. In [124] also a high deposition rate is reported for sputtering of a TiO_x ($1.5 < x < 1.7$) target in pure Ar. In [119] the deposition rate of TiO_{2-x} in pure Ar is reported to be 6 times that of the rate in the reactive mode. It seems that, when sputtered in pure Ar, the oxide target operates in the transition region of the metallic target [125], and it is possible to deposit stoichiometric films under these conditions [30, 126]. With increasing oxygen flow the same sputtering conditions as for the metallic target in the reactive sputtering mode are reached [125]. For TiO_{2-x} targets no unstable sputtering regime is observed [22, 122, 125], so that high rate deposition of stoichiometric films does not require sophisticated process control [123, 124].

5.2. Structural development during film growth

A well known and much referred to model for the microstructural development during thin film growth by metal evaporation is the one developed Movchan and Demchishin [127], which was extended to sputtering by Thornton [128]. Latter describes the changes in microstructure observed when depositing thick (metallic) films with the substrate temperature T_s (referred to the melting temperature T_m), and the inert gas pressure as parameters. According to the observed thin film structure the growth was divided into different zones. The Thornton model was further developed by [129] relating the different zones to the particle energy instead of the surface temperature. It is beyond the scope of our review to discuss this structure zone model in detail, but we will give a summary here and point out how it can be used to define the deposition conditions for thin film structures that are of interest for depositing photocatalytic TiO_2 films.

In the structure zone model by [129] the thin film growth is divided into three different growth zones (1-3), with an intermediate zone T between zone 1 and zone 2. In zone 1 the particle energy on the substrate surface is too low to allow diffusion. For very low particle energies a so-called *hit-and-stick* growth occurs, which results in amorphous or nanocrystalline, highly porous and finely grained films. With increasing particle energy kinetic crystal growth can occur in this zone 1, but the film density remains low. From zone T on the arriving particles have enough energy to move on the substrate surface, so that

preferential crystal growth can occur. As a result, the film density and the size of the single crystal grains increase. In zone 3 the particle energy is high enough to allow bulk diffusion, which should ultimately lead to the growth of a single crystal film. The presence of defects and impurities prevents this due to the formation of grain boundaries, though [129].

The important issues for depositing photocatalytic TiO_2 are crystallinity, stoichiometry (degree of oxidation), density and surface morphology. From the description of the structure zones it becomes clear that zone 1, and to some extent zone T, are the most interesting for photocatalytic TiO_2 thin film growth. The low density and small grain size will increase the surface area of the thin film (section 3.6), enhancing its photocatalytic activity.

5.3. Controlling the structure of TiO_2 thin films

As already discussed in section 3.1 the rutile phase is the thermodynamically stable one, but since the energies of the anatase and brookite phases are only slightly higher, they can exist as metastable phases up to the transformation temperature of about 800°C [4]. For the grain sizes below about 15 nm anatase is more stable than rutile or brookite, so that the crystal phase formed can be controlled by the grain size.

The discussion of the thin film growth using the structure zone model (section 5.2) becomes more complex in the case of TiO_2 for two reasons: (i) one has to take into account different crystal phases possible and (ii) the sputtering process is reactive so that the oxygen partial pressure is an additional parameter. In the following we give a short summary of the different deposition conditions used to obtain rutile, anatase or amorphous TiO_2 films with reactive (d.c.) magnetron sputtering. No reference to the growth of brookite films using (d.c.) magnetron sputtering was found.

Under most standard sputtering conditions and the substrate at room temperature the particles forming the thin film remain quasi immobile on the film surface so that the films follow the zone 1 type growth. This means that the TiO_2 films are either XRD amorphous (section 3.2.1) or show only a very low degree of crystallinity [130]. D.c. sputtering almost exclusively leads to the deposition of the amorphous or the anatase structure, while pulsed d.c. and r.f. sputtering can also yield rutile or mixed anatase/ rutile structures. For the latter techniques the energy received by the growing film per incoming particle is higher at the same input power, due to a lower deposition rate as well as a higher degree of ionization in the plasma. As a result, a higher substrate self heating [114, 131] is observed. When crystalline films are deposited very often a preferential orientation is observed, which may vary according to the deposition conditions.

The energy of the particles arriving at the substrate is mostly determined by the sputter gas pressure and the target-to-substrate distance [114]. Both

control the extent of particle collision in their path between target and substrate: Each collision leads to energy loss, and the number of collisions increases with increasing pressure and target-to-substrate distance. Important is also the oxygen partial pressure because (i) the deposition rate decreases with increasing oxygen flow rate, remaining stable once the reactive mode is established and (ii) the discharge voltage increases strongly upon transition from the metallic to the reactive mode (when using metallic Ti targets). The former decreases the energy received by the growing film per unit time while the latter increases the energy per arriving particle. An additional factor is the increase in substrate temperature either due to external heating or self heating during the process. The total energy deposited in the thin film can additionally be varied by the number of incoming particles per unit time. Latter is varied by the sputter rate, which itself depends mostly on the discharge current [114]. Another method to increase the energy of the particles bombarding the thin film is by using so-called' unbalanced' magnetron sputtering [129]. Here the magnetic field lines direct the flux of charged particles present in the plasma to the substrate, delivering additional energy to the growing film.

From the above discussion one can expect that rutile films are formed for higher particle energies combined with a low deposition rate. Both result in larger grain sizes, allowing the thermodynamically stable phase to form. This is confirmed by experimental results for r.f., a.c. or pulsed d.c. sputtering given in [132-136]. Very recently it was reported that an almost pure rutile film was obtained using d.c. magnetron sputtering [137]. On the other hand, amorphous or nanocrystalline films are expected to form at low particle energies and low substrate temperatures, which is confirmed by experimental results [32, 132, 135, 136, 138-140].

Anatase is reported to form at medium particle energies, especially when smaller grains are formed. Elevated substrate temperatures will enhance crystallization, but one needs to keep in mind that temperatures above 800°C almost exclusively result in the crystallization of rutile as well as strong grain growth [4]. For r.f. sputtering the formation of anatase falls between the conditions listed for rutile and amorphous TiO_2. For d.c. sputtering it was found that the crystallization of anatase was promoted by increasing the arriving particle energy [32, 138, 139-142]. The results indicate that there is no difference using Ti and TiO_{2-x} as target material.

5.4. Important issues for improving the photocatalytic activity

Up to now the highest photocatalytic activity has been reported for anatase or anatase/ rutile mixed phases, so that the obvious aim is to deposit such structures. The disadvantages of depositing crystalline thin films are the larger grain size due to crystal growth and the elevated deposition temperatures

needed. Our own studies have shown that amorphous thin films can have a quite high photocatalytic activity when their porosity is larger than 20% [30]. Such films have a low grain diameter of 50 nm, which increases their active surface area (section 3.6). Since they are deposited at temperatures below 50°C it is possible to deposit them on heat sensitive substrates. Amorphous films can be crystallized by an anneal treatment at temperatures between 300 and 400°C [30, 143, 144]. These temperatures are too low for grain growth so that the fine grain size of the as deposited coating is preserved.

6. Measuring the photocatalytic activity of TiO_2 thin films

In order to determine the activity of a photocatalyst it is necessary to have an experimental procedure to either directly measure the conversion of light energy into the lowering of the activation energy of a given breakdown reaction or to compare the evolution of a chemical reaction between different catalysts and/ or organic substances. The former is rather difficult, if not impossible to measure directly, while the latter gives only indirect evidence of the catalyst activity. In this paragraph we point out the special considerations for determining the photocatalytic activity of a thin film.

Figure 12. (left) shows the sketch of a generic setup for measuring the photocatalytic activity of a thin film catalyst. The concentration of the organic test substance (OR) and, if desired, of the decomposition product(s) (DP) are followed by the analyzer for example a gas chromatograph (GC), a mass spectrometer (MS) or a photo-spectrometer. Figure 12. (right) shows the evolution of the OR and the DP for the case of first order reaction kinetics. Normally the initial rate of the breakdown reaction (taken from the initial slope of the concentration of the organic as a function of time) is used as a measure for the catalytic activity of the thin film [145]. It can therefore be interesting to change the order of the reaction to zero as this results in an initially linear

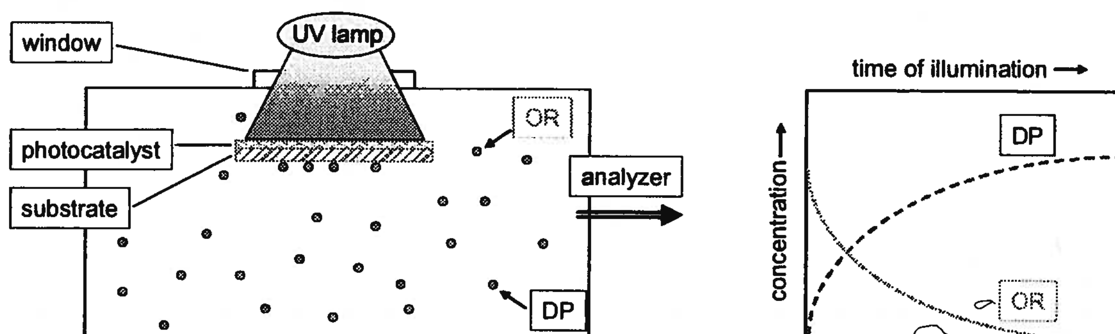

Figure 12. Sketch of a generic measurement setup to follow the photocatalytic breakdown of an organic substance (OR) and its decomposition product (DP).

decay of the OR concentration [8]. It is a rather complex procedure to determine the efficiency of a photocatalyst quantitatively. Standard definitions and procedures were established by the IUPAC [145, 146] for the testing of the photocatalytic activity of a powder suspended in water. These procedures are designed to report the absolute photocatalytic activity of a given TiO_2, referenced to the number of active photons (UV) arriving at the powder surface.

Unfortunately the suggested reference organic compounds (phenol as aromatic and formic acid as aliphatic organic) are not very suitable for testing in a gaseous environment [145]. Additionally, the true surface area of a thin film is usually not measurable (section 3.6.1), even though it can be estimated using the procedure outlined in section 3.6.2. As a result, most experimental settings for testing thin film photocatalysts are not compatible with the strict requirements stated by the IUPAC, meaning that a more qualitative approach must be applied. One option is to use a reference thin film catalyst against which other thin films, organic substances or changes in the experimental settings can be tested. The major problem is, though, that no universally available TiO_2 thin film catalyst material exists. The only reports of a reference thin film were found in [47, 147], where a spin coated layer of the well-known powder catalyst Degussa P25 was used. A second suggested material was Pilkington Active™ [47], a CVD deposited thin film on SiO_2 coated glass, but this material has a very low photocatalytic activity due to is low thickness [31].

There are several important parameters when testing and comparing thin film photocatalysts. The first is the number of (active) photons (i.e. the UV intensity) absorbed in the thin film. This number depends on the film thickness (section 3.7), the spectral range and power of the (UV) lamp used and how much light is lost between lamp and thin film surface. The second parameter is the initial concentration of the organic test substance in relation to the active thin film surface area, which determines the coverage of the catalyst surface and therefore the reaction kinetics [4, 8]. The third parameter is the nature of the organic test substance, which determines the active pore size and therefore the active surface area of the thin film. Additional parameters are the degree of surface hydroxylation (section 3.4) and the presence of oxygen. Latter is normally taken care of by working in air or by supplying a surplus of oxygen to the reaction chamber (e.g. by bubbling).

7. Conclusions and outlook

In this review we discussed several aspects of TiO_2 thin film deposition for photocatalytic applications. We started with the factors influencing the photocatalytic activity of TiO_2 thin films, the two most important being the microstructure and the crystallinity. Even though the active surface area is one

of the most important factors for a catalyst, the effect of the microstructure on the photocatalytic activity is neglected in most studies on thin films. In this review we demonstrated how the microstructure (porosity) of the thin films can enlarge the surface area. Next to keeping the grain size small it is important to estimate the pore size of the thin film and to determine whether these pores are large enough to enable inward diffusion of the organic substance studied and outward diffusion of reaction products. Additionally the thickness of the thin film is important, especially for high porosity, because the depth of the pores and, as a result, the active film surface area increases.

The thin film crystallinity is the other important factor. Crystalline defects can act as trap sites for the photogenerated charge carriers, reducing the number of charge carriers available for the reaction to be catalyzed. For high crystallinity it is interesting to minimize the number of grain boundaries, i.e. to increase the grain size. This is contrary to the desire to increase the surface area, so that usually a grain size range of about 10-20 nm is considered an optimum compromise between these two issues. From the three most common TiO_2 crystalline phases anatase is reported to be the most photoactive one. This is one of the reasons why most studies work with crystalline anatase thin films. Anatase is also the crystal phase which forms most easily for small grain sizes and at the processing conditions commonly used.

TiO_2 thin films can be deposited with a variety of techniques based on wet chemical and vapor deposition techniques. The most popular ones are sol-gel, chemical vapor deposition (CVD), and magnetron sputtering, a physical vapor deposition (PVD) technique. Independent of the deposition technique used it is desirable to control the deposition parameters as to yield thin films that fulfill the two basic requirements of high surface area and good crystallinity. For many techniques crystalline thin films can only be obtained when heated during or after deposition. This limits the substrate material choice, with most polymers not being applicable. Additionally, uptake of sodium or other detrimental contaminants from the substrate must be avoided. An alternative can be to deposit a thin film of low crystallinity at low temperatures and optimize its microstructure as to yield a high surface area.

Unfortunately there is no standard procedure or reference sample for measuring the photocatalytic activity of TiO_2 thin films. This makes it difficult to compare results between laboratories or different measurement setups. We think that this issue is an important one for the future.

8. References

1. Fujishima A., Honda K. 1972, Nature 238, 37.
2. Schiavello M. 1997, Heterogeneous photocatalysis, Wiley Series in Photoscience and Photoengineering, Volume 3, John Wiley & Sons, Chichester.
3. Anpo M., Takeuchi M. 2003, J. Catal. 216, 505.

4. Carp O., Huisman C.L., Reller A. 2004, Prog. Solid State Chem. 32, 33.
5. Fernández-García M.,. Martínez-Arias A, Hanson J.C., Rodriguez J.A. 2004, Chem. Rev. 104, 4063.
6. Fujishima A., Rao T.N., Tryk D.A. 2000, J. Photochem. Photobio. C: Photochem. Rev. 1, 1.
7. Linsebigler A.L., Lu G., Yates Jr J.T. 1995, Chem. Rev. 95, 735.
8. Mills A., Le Hunt S., J. 1997, Photochem. Photobio. A: Chem. 108, 1.
9. Karches M., Morstein M., von Rohr P.R., Pozzo R.L., Giombi J.L., Baltanás M.A. 2002, Catal. Today 72, 267.
10. Boulesteix C., Kang Z., Lottiaux M. 1986, Phys. Stat. Sol. (a) 94, 499.
11. Takeda S., Suzuki S., Odaka H., Hosono H. 2001, Thin Solid Films 392, 338.
12. Nam H.-J., Amemiya T., Murabayashi M., Itoh K. 2004, J. Phys. Chem. B 108, 8254.
13. Fallet M., Permpoon S., Deschanvres J.L., Langlet M. 2006, J. Mater. Sci. 41, 2915.
14. Smith D.L. 1995, Thin Film Deposition, Principles and Practice, Chap. 5: Deposition, McGraw-Hill, Inc., New York, 119.
15. Eufinger K. 2007, PhD Thesis, Ghent University, Ghent, Belgium.
16. Damm C., Völtzke D., Abicht H.-P., Israel G. 2005, J. Photochem. Photobio. A: Chem. 174, 171.
17. Yin S., Hasegawa H., Maeda D., Ishitsuka M., Sato T. 2004, J. Photochem. Photobio. A: Chem. 163, 1.
18. Miyagi T., Kamei M., Mitsuhashi T., Ishagashi T., Yamazaki A. 2004, Chem. Phys. Lett., 390, 399.
19. Ohno T., Sarukawa K., Tokieda K., Matsumura M. 2001, J. Catal. 203, 82.
20. Ohno T., Tokieda K., Higashida S., Matsumara M. 2003, Appl. Cat. A: General 244, 383.
21. Zallen R., Moret M.P. 2006, Solid State Commun. 137, 154.
22. Kominami H., Ishii Y., Kohno M., Konishi S., Kera Y., Ohtani B. 2003, Catal. Lett. 91, 41.
23. J.I. Pankove1971, Optical processes in semiconductors, Dover Publications, Inc., New York.
24. Jung K.Y., Park S.B. 1999, J. Photochem. Photobio. A: Chem. 127, 117.
25. Jung K.Y., Park S.B., Ihm S.-K. 2002, Appl. Cat. A: General 224, 229.
26. Jung K.Y., Park S.B. 2004, Mater. Lett. 58, 2897.
27. Baroch P., Musil J., Vlcek J., Nam K.H., Han J.G. 2005, Surf. Coat. Technol. 193, 107.
28. Hove M.A. 2006, Catal. Today 113, 133.
29. Zeman P., Takabayashi S. 2003, Thin Solid Films 433, 57.
30. Eufinger K., Poelman D., Poelman H., De Gryse R., Marin G.B. 2007, Vac. Technol. Coat. 8, 44.
31. Eufinger K., Poelman D., Poelman H., De Gryse R., Marin G. B. 2007, J. Phys. D: Appl. Phys. 40, 5232.
32. Liu B., Zhao X., Zhao Q., Li C., He X. 2005, Mater. Chem. and Phys. 90, 207.
33. Zhang W., Li Y., Zhu S., Wang F. 2004, Chem. Phys. Lett. 373, 333.
34. Asahi R., Morikawa T., Ohwaki T., Aoki K., Taga Y. 2001, Science 293, 269.

35. Ihara T., Miyoshi M., Iriyama Y., Matsumoto O., Sugihara S. 2003, Appl. Cat. B: Environ. 42, 403.
36. Prabakar K., Takahashi T., Nezuka T., Nakashima T., Kubota Y., Fujishima A. 2006, J. of Vac. Sci. and Technol. A 24, 1156.
37. Miyagi T., Kamei M., Mitsuhashi T., Yamazaki A. 2006, Appl. Phys. Lett. 88, Artn 132101.
38. Wang Y., Doren D.J. 2005, Solid State Commun. 136, 186.
39. Mathieu H., Pascual J., Camassel J. 1978, Phys. Rev. B 18, 6920.
40. Miao L., Tanemura S., Watanabe H., Toh S., Kaneko K. 2005, Appl. Surf. Sci. 244, 412.
41. Wunderlich W., Oeckermann T., Miao L., Hue N.T., Tanemura S., Tanemura M. 2004, J. Ceram. Process. Res. 5, 343.
42. Wunderlich W., Miao L., Tanemura M., Tanemura S., Jin P., Kaneko K., Terai A., Nabatova-Gabin N., Belkada R. 2004, Int. J. Nanosci. 3, 439.
43. Anderson O., Ottermann C.R., Kuschnereit R., Hess P., Bange K. 1997, Fresenius J. Anal. Chem. 358, 315.
44. Fernández A., Lassaletta G., Jiménez V.M., Justo A., González-Elipe A.R., Herrmann J.-M., Tahiri, H. Ait-Ichou Y. 1995, Appl. Cat. B: Environ. 7, 49.
45. Tada H., Tanaka M. 1997, Langmuir 13, 360.
46. Tomaszewski H., Eufinger K., Poelman H., Poelman D., De Gryse R., Smet P.F., Marin G.B. 2007, Int. J. Photoenergy 8, ID 95213.
47. Mills A., Lepre A., Elliot N., Bhopal S., Parkin I.P., O'Neill S.A. 2003, J. Photochem. Photobio. A: Chem. 160, 213.
48. Guan K. 2005, Surf. Coat. and Technol. 191, 155.
49. Sakthivel S., Hidalgo M.S., Bahnemann D.W., Geissen S.-U., Murugesan V., Vogelpohl A. 2006, Appl. Cat. B: Environ. 63, 31.
50. Cornu C.J.G. 2002, PhD Thesis, California Institute of Technology, Pasadena, California.
51. Tjong S.C., Chen H. 2004, Mater. Sci. Eng. R 45, 1.
52. Li W., Ismat Shah S., Huang C.-P., Jung O., Ni C. 2002, Mater. Sci. Eng. B 96, 247.
53. Dumitriu D., Bally A.R., Ballif C., Hones P., Schmid P.E., Sanjinés R., Lévy F., Pârvulescu V.I. 2000, Appl. Cat. B: Environ. 25, 83.
54. Madhusudan Reddy K., Manorama Sunkara V., Ramachandra Reddy A. 2002, Mater. Chem. Phys. 78, 239.
55. Monticone S., Tufeu R., Kanaev A.V., Scolan E., Sanchez C. 2000, Appl. Surf. Sci. 162-163, 565.
56. Baklanov M.R., Moglinov K.P., Polovinkin V.G., Dultsev F.N. 2000, J. Vac. Sci. Technol. B 18, 1385.
57. Poelman D., Smet P.F. 2003, J. Phys. D: Appl. Phys. 36, 1850.
58. http://en.wikipedia.org/wiki/Mesopore, /Macropore, /Micropore.
59. Eufinger K., Poelman D., Poelman H., De Gryse R., Marin G. B. 2007, Appl. Surf. Sci. 254, 148.
60. Jung S.-C., Kim S.-J., Imaishi N., Cho Y.-I. 2005, Appl. Cat. B: Environ. 55, 253.
61. Kern P., Schwaller P., Michler J. 2006, Thin Solid Films 494, 279.

62. An H.J, Jang S.R., Vittal R., Lee J., Kim K.J. 2005, Electrochim. Acta, 50, 2713.
63. Manivannan A., Spataru N., Arihira K., Fushishima A. 2005, Electrochem. Solid-State Lett. 8, 138.
64. Georgieva J., Armyanov S., Valova E., Poulios I., Sotiropoulos S. 2006, Elechtrochim. Acta 51, 2076.
65. Yan H.W., Yang Y.L., Fu Z.P., Yang B.F., Xia L.S., Xu Y.D., Fu S.Q., Li F.Q. 2006, Chem. Lett. 35, 864.
66. Karuppuchamy S., Jeong J.M., Amalnerkar D.P., Minoura H. 2006, Vacuum 80, 494.
67. Ishikawa Y., Matsumoto Y. 2002, Solid State Ionics 151, 213.
68. Wessels K., Feldhoff A., Wark A., Rathhousky J., Oekermann T. 2006, Elechtrochem. Solid-State Lett. 9, C93.
69. Sankapal B.R., Sartale S.D., Lux-Steiner M.C., Ennaoui A. 2006, C.R. Acad. Sci., Ser. IIc: Chim. 9, 702.
70. Zotti G., Schiavon G., Zecchin S. 1999, J. Electrochem. Soc. 146, 637.
71. Backman U., Auvinen A., Jokiniemi J.K. 2005, Surf. Coat. Technol. 192, 81.
72. Kim B.H., Lee J.Y., Choa Y.H., Higuchi M., Mitzutani N. 2004, Mater. Sci. Eng. B 107, 289.
73. Woo K., Lee W.I., Lee J.S., Kang S.O. 2003, Inorg. Chem. 42, 2378.
74. Sato N., Nakajima K., Usami N., Takahashi H., Muramatsu A., Matsubara E. 2002, Mater. Transact. 43, 1533.
75. Besserguenev V.G., Pereira R.J.F., Mateu M.C.s, Khmelinskii I.V., Nicula R.C., Burkel E. 2003, Int. J. Photoenergy 5, 99.
76. Jung C.K., Lee S.B., Boo J.H., Ku S.J., Yu K.S., Lee J.W. 2003, Surf. Coat. Technol. 174, 296.
77. Amassian A., Svec M., Desjardins P., Martinu L. 2006, J. Vac. Sci. Technol. A 24, 2061.
78. Horakova M., Kolouch A., Spatenka P. 2006, Chech. J. Phys. 56, B1185.
79. Kambe M., Fukawa M., Taneda N., Sato K. 2006, Sol. Engergy Mater. Sol. Cells 90, 3014.
80. Borras A., Barranco A., Gonzalez-Elipe A.R. 2006, J. Mater. Sci. 41, 5220.
81. Sonnenfeld A., Hauert R., von Rohr P.R. 2006, Plasma Chem. Plasma Process. 26, 319.
82. Maeda M., Watanabe T. 2005, Thin Solid Films, 489, 320.
83. Hatanaka Y., Naito N., Itou S., Kando M. 2005, Appl. Surf. Sci. 244, 554.
84. Ahn K.H., Park Y.B., Park D.W. 2003, Surf. Coat. Technol. 171, 198.
85. Huang S.S., Chen J.S. 2002, J. Mater. Sci. - Maters Eletron. 13, 77.
86. Nakamura M., Kato S., Aoki T., Sirghi L., Hatanaka Y. 2001, Thin Solid Films 401, 138.
87. Martinu L., Poltras D. 2000, J. Vac. Sci. Technol. A 18, 2619.
88. Ando Y., Tobe S., Tahara H. 2006, Vacuum 80, 1278.
89. Goto T., Kimura T. 2006, Science of Engineering Ceramics III, Series on Key Engineering Materials, 317-318, 495.
90. Halary-Wagner E., Wagner F.R., Brioude A., Mugnier J., Hoffmann P. 2005, Chem. Vap. Deposition 11, 29.
91. Zhang J.Y., Boyd I.W., O'Sullivan B.J., Hurley P.K., Kelly P.V., Senateur J.P. 2002, J. Non-Cryst. Sol. 303, 134.

92. Simcock M.N. 2006, Surf. Interface Anal. 38, 1122.
93. No S.Y., Oh J.H., Jeon C.B., Schindler M., Hwang C.S., Kim H.J. 2005, J. Electrochem. Soc. 152, C435.
94. Conde-Gallardo A., Guerrero M., Fragoso R., Castillo N. 2006, J. Mater. Res. 21, 3205.
95. Nolan M.G., Pemble M.E., Sheel D.W., Yates H.M. 2006, Thin Solid Films 515, 1956.
96. Richards B.S., Huong N.T.P., Crosky A. 2005, J. Electrochem. Soc. 152, F71.
97. Lim G.T., Kim D.H. 2006, Thin Solid Films 498, 254.
98. Kim S.K., Kim K.M., Kwon O.S., Lee S.W., Jeon C.B., Park W.Y., Hwang C.S. 2005, J. Jeong, Electrochem. Solid-State Lett. 8, 59.
99. Pore V., Rathu A., Leskela M., Ritala M., Sajavaara D., Keinonen J. 2004, Chem. Vap. Deposition 10, 143.
100. Mitchel D.R.G., Attard D.J., Triani G. (2003), Thin Solid Films 441, 85.
101. Schuisky M., Aarik J., Kukli K., Aidla A., Harsta A. 2001, Langmuir 17, 5508.
102. Rao K.N. 2002, Opt. Eng. 41, 2357.
103. Selhofer H., Ritter E., Linsbod R. 2002, Appl. Opt. 41, 756.
104. Li C.R., Zheng Z.H., Zhang F.M., Yang S.Q., Wang H.M., Chen L.Z., Zhang F., Wang X.H., Liu X.H. 2000, Nucl. Instr. Method. Phys. Res. B 169, 21.
105. Chen H.C., Lee C.C., Jaing C.C., Shiao M.H., Lu C.J., Shieu F.S. 2006, Appl. Opt. 45, 1979.
106. Modes T., Scheffel B., Metzner C., Zywitzki O., Reinhold E. 2005, Surf. Coat. Technol. 200, 306.
107. Jiang J.C., Li B., Zhang Z.Q., Hu P.G., Zhang F.S., Cheng H.S., Yang F.J. 2002, Phys. Sta. Sol. (a) 193, 69.
108. Yang T.S., Shiu C.B., Wong M.S. 2004, Surf. Sci. 548, 75.
109. Tien C.L., Lin S.W. 2006, Optics. Commun. 266, 574.
110. Guo A.Y., Xue Y.Y., Zhu X.M., Zhang G.Y., Guo P.T., Hu X.F. 2006, J. Wuhan. Univ. Technol. - Mater. Sci. Ed. 21, 101.
111. Chambers S.A. 2000, Surf. Sci. Rep. 39, 105.
112. Chapman B.N. 1980, Glow Discharge Processes, John Wiley & Sons, New York.
113. Vossen J.L., Cuomo J.J. 1978, Thin film processes Pt. 2, chapter II-1, Vossen J.L., Kern W. (ed.), Academic Press.
114. Westwood W. 2003, Sputter deposition, AVS Education Committee Book Series, Volume 2.
115. Waits R.K. 1978, Thin film processes Pt. 2, chapter II-4, Vossen J.L., Kern W. (ed.), Academic Press.
116. Berg S., Nyberg T. 2005, Thin Solid Films 476, 215.
117. Safi I. 2000, Surf. Coat. Technol. 127, 203.
118. Sproul W.D., Christy D.J., Carter D.C. 2005, Thin Solid Films 491, 1.
119. Ohsaki H., Tachibana Y., Hayashi A., Mitsui A., Hayashi Y. 1999, Thin Solid Films, 351, 57.
120. Ohsaki H., Tachibana Y., Mitsui A., Kamiyama T., Hayashi Y. 2001, Thin Solid Films 392, 169.
121. Tachibana Y., Ohasaki H., Hayashi A., Mitsui A., Hayashi Y. 2000, Vacuum 59, 836.

122. Tomaszewski H., Poelman H., Depla D., Poelman D., De Gryse R., Fiermans L., Reyniers M.F., Heynderickx G., Marin G.B. 2003, Vacuum 68, 31.
123. Poelman H., Tomaszewski, H. Poelman D., Depla D., De Gryse R. 2004, Surf. Interface Anal. 36, 1167.
124. Persoone P., Diericks S., Luys S., De Bosscher W. 2005, Proc. 48th Ann. Tech. Conf. Soc. of Vacuum Coat. (SVC), Denver, Co, 180.
125. Depla D., Tomaszewski H., Buyle G., De Gryse R. 2006, Surf. Coat. Technol. 201, 848.
126. Eufinger K., Janssen E.N., Poelman H., Poelman D., De Gryse R., Marin G.B. 2006, Thin Solid Films 515, 425.
127. Monchavan B.A., Demchishin A.V. 1969, Phys. Met. Metallogr. 28, 83.
128. Thornton J. A. 1977, Ann. Rev. Mater. Sci. 7, 239.
129. Mahieu S., Ghekiere P., Depla D., De Gryse R. 2006, Thin Solid Films 515, 1229.
130. Baroch P., Musil J., Vlček J., Nam K.H., Han J.G. 2005, Surf. Coat. Technol. 193, 107.
131. Snyders R., Gouttebaron R., Dauchot J.P., Hecq M. 2005, Surf. Coat. Technol. 200, 448.
132. Asanuma T., Matsutani T., Liu C., Mihara T., Kiuchi M. 2003, Proc. 7th Int. Symp. Sputt. Plasma Proc. (ISSP 2003), Kanazawa Inst. Technol., Kanazawa, Japan, 447.
133. Miao L., Jin P., Kaneko K., Tanemura S. 2002, Proc. Advanced Nanomater. Nanodevices (IUMRS-ICEM), Xi'an, China, 943.
134. Okimura K. 2001, Surf. Coat. Technol. 135, 286.
135. Yamagishi M., Kuriki S., Shigesato Y. 2003, Thin Solid Films 442, 227.
136. Zeman P., Takabayashi S. 2002, Surf. Coat. Technol. 153, 93.
137. Vale A., Chaure N., Simonds M., Ray A.K., Bricklebank N. 2006, J. Mater. Sci. - Mater. Electron. 17, 851.
138. Barnes M.C., Kumar S., Green L., Hwang N.-M., Gerson A.R. 2005, Surf. Coat. Technol. 190, 321.
139. Kim S.-H., Choi Y.-L., Song Y.-S., Lee D. Y., Lee S.-J. 2002, Mater. Lett., 57, 343.
140. Takahashi T., Prabakar K., Nezuka T., Yamazaki T., Nakashima T., Kubota Y., Fujishima A. 2006, J. Vac. Sci. Technol. A 24, 1161.
141. Zhang W., Li Y., Zhu S., Wang F. 2004, Surf. Coat.s Technol. 182, 192.
142. Takahashi T., Nakabashi H., Mizuno W. 2002, J. Vac. Sci. Technol. A 20, 1916.
143. Martin N., Rousselot C., Rondot D., Palmino F., Mercier R. 1997, Thin Solid Films 300, 113.
144. Zheng S.K., Wang T.M., Xiang G., Wang C. 2001, Vacuum 62, 361.
145. Serpone N., Salinaro A. 1999, Pure Appl. Chem. 71, 303.
146. Salinaro A., Emeline A.V., Zhao J., Hidaka H., Rybabchuk V.K., Serpone N. 1999, Pure Appl. Chem. 71, 321.
147. Mills A., Elliot N., Parkin I.P, O'Neill S., Clark R. J. 2002, J. Photochem. Photobio. A: Chem. 151, 171.